Investigation on the sensing performances of strip and rib SOI waveguides microring structures

Deng Lili[1,2], Shi Qiang[1,2], Zhang Hui[1,2], Duan Qianqian[1,2], Jian Aoqun[1,2], Sang Shengbo[1,2], Zhang Wendong[1,2]

(1. MicroNano System Research Center, Taiyuan University of Technology, Taiyuan 030024, China;
2. Key Laboratory of Advanced Transducers and Intelligent Control System, Shanxi Province and Ministry of Education, Taiyuan 030024, China)

Abstract: The strip and rib waveguides based on silicon-on-insulator (SOI) microring resonator structures are investigated by the Finite Difference Time Domain (FDTD) method. The theory of microring resonators used in biosensing was explored. The effects of geometric structure dimension on biosensor sensitivity were considered and analyzed. It is demonstrated that the sensitivity of strip waveguide is much higher than that of rib waveguide, which is proved by their mode field distributions, and the sensitivity coefficients of both strip and rib waveguides have the similar trend with the increase of waveguide width. Furthermore, the strip waveguide has the highest sensitivity coefficient when the cross section is square, whereas that of rib waveguide corresponds to a not totally symmetrical geometry. The maximum sensitivity of strip waveguide is 172.3 nm/RIU when the cross section is fully symmetry.

Key words: strip and rib waveguides; microring resonator; biosensor; cross section
CLC number: TN302 Document code: A Article ID: 1007-2276(2015)02-0752-06

条形和脊型 SOI 波导微环结构传感性能研究

邓丽莉[1,2],石 强[1,2],张 辉[1,2],段倩倩[1,2],菅傲群[1,2],桑胜波[1,2],张文栋[1,2]

(1. 太原理工大学 微纳系统研究中心,山西 太原 030024;
2. 太原理工大学 新型传感器与智能控制教育部和山西省重点实验室,山西 太原 030024)

摘 要:使用时域有限差分(FDTD)方法研究了基于 SOI 微环谐振腔结构的条形和脊型波导,探究了微环谐振腔应用于生物传感的理论。分析了结构的几何尺寸对生物传感器灵敏度的影响。通过分析条形和脊型波导的模场分布图,解释了条形波导的灵敏度明显高于脊型波导的原因,且随着波导宽度的增加其灵敏度系数的变化遵循相同的趋势。并且,当条形波导取得最高的灵敏度系数时,其横截面是

收稿日期:2014-06-10; **修订日期**:2014-07-13
基金项目:国家自然科学基金(91123036,51105267);高等学校博士学科点专项科研基金(20131402110013,20111402120007);
山西省科技厅科技重大专项(20121101004);山西省高等学校特色重点建设学科项目(晋教材[2012]45 号);
山西省回国留学人员科技活动项目择优资助项目
作者简介:邓丽莉(1990-),女,硕士生,主要从事纳米光波导耦合谐振腔方面的研究。Email:denglili1990@sina.com
导师简介:桑胜波(1979-),男,副教授,硕士生导师,博士,主要从事微纳传感器与纳米光波导集成器件的研究。
Email:sangshengbo@tyut.edu.cn

方形的,然而脊型波导的最大灵敏度值对应的却是不完全对称的几何结构。当条形波导的横截面全对称时,灵敏度达到最大值 172.3 nm/RIU。

关键词:条形和脊型波导; 微环谐振腔; 生物传感器; 横截面

0 Introduction

In recent years, silicon optical device, which has great potential in batch production, has attracted growing concern and research efforts owing to its compatible fabrication process with complementary metal-oxide-semiconductor(CMOS) technology[1-2]. Microring resonator is one of the most common and important structures among silicon devices, and has played a key role in the development of silicon photonics research[3]. A typical SOI-based microring resonator consists of a ring waveguide and a bus waveguide, which are very close to each other[4]. Due to the high refractive index difference between the silicon core (3.5) and silica substrate (1.45), the physical dimension of the microring can be reduced to a submicron level, so that the ultra-compact silicon photonic integration could be achieved on a SOI chip[5].

Microring resonators based optical biosensors possess wide applications in biomedical research because of the characteristics of label free detection and high sensitivity[6-8]. The detection principle is that the effective refractive index of the waveguide will change when different samples bind on the waveguide surface, which will further affect the transmission spectrum at the output side of the bus waveguide[9]. To enhance the biosensing performance, many research efforts have been poured into improving the sensitivity of the device. Generally speaking, there are two ways to improve the sensitivity of the sensor based on microring resonator. One is to reduce the area of the cross section, because smaller cross section makes a stronger evanescent field outside the waveguide for sensing [10]. However, as the dimension of waveguide cross section decreases, the difficulty of etching process increases significantly[11]. Furthermore, the surface roughness of waveguide will also become larger, thus further influencing the performance and integration of sensors[12]. The other method is to optimize the structure of mirroring resonator[13], of which the design of cross section is a crucial point.

In this paper, the theory of biosensing utilizing SOI microring structures is analyzed, and a brief introduction of the processing technology is provided. Then, two geometry designs of the microring structures (cross section)——strip and rib waveguides, are investigated. For each design, different sets of the design parameters (e.g. width and thickness of the waveguides) are analyzed and optimum parameters are revealed based on the FDTD simulation results. Furthermore, for specific values of cross-sectional area, the highest sensitivities of the two SOI microring sensors are obtained, respectively. Finally, the comparisons of sensitivity, mode field distributions and other characteristics between the two structures are presented.

1 Theory and analysis

The strip waveguide and the rib waveguide are very favorable in microring resonator devices, because their large surface areas are apt for specific modification and can be used for the binding of events[14]. For comparison, the slot waveguide, however, has the similar dimension structure[10] but little sensing performance difference to the strip and rib waveguides. Moreover, without controlling the slot width accurately, the etching process of strip or rib waveguide is relatively simple than slot waveguide. Additionally, in sensor applications, the sidewall roughness of waveguide caused by etching[15] can be reduced by electron beam lithography (EBL), inductively coupled plasma (ICP) etching techniques and hydrogen annealing process. In

terms of EBL, the electron beam (EB) scanning step, layout design, exposure dose can be chosen properly to further smooth the waveguide sidewall. For the ICP, the roughness can also be decreased by increasing the ratio of physical and chemical etching[16]. And the waveguide roughness can also be removed by annealing in hydrogen under high temperature within certain time[17-18]. Hence, in order to improve the performance of sensors, apart from taking the above factors into consideration, the designs of cross sections of the waveguides, including rib and strip, are essential, and their performance in sensing needs to be compared and optimized. The designs of the rib and strip waveguides are schematically shown in Fig.1(a) and (b), respectively, where h_{rib} is the ridge height of the rib waveguide, h_{strip} is the thickness of the strip waveguide, w is the core width of the rib waveguide and strip waveguide. The cumbersome calculation is simplified but representative maintained.

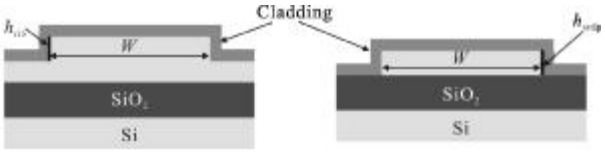

(a) (b)

Fig.1 Cross section of a rib waveguide and a strip waveguide

In this paper, we monitored the shift of resonant wavelength in biosensing. As light couples into the microring and interferes in the coupling region, a series of resonance dips can be observed at the output spectrum[19]. When some biomolecules(refractive index= n_e) are bound on the cladding of the microring, the effective refractive index of microring becomes n_{eff}. As shown in Eq. (1), the resonant wavelength λ is dependent on the effective refractive index of microring n_{eff},

$$2\pi R n_{eff} = m\lambda \quad (1)$$

where R is the bending radius of the microring, and m is the interference order[20].

For single ring structure, according to Eq.(1), the shift of the resonant peak $\Delta\lambda$ due to the change of the effective refractive index of microring n_{eff} can be expressed as:

$$\Delta\lambda = \frac{\Delta n_{eff}}{n_{eff}}\lambda \quad (2)$$

In this sensing theory, the microring sensitivity is given by Eq.(3)[21]:

$$S = \frac{\Delta\lambda}{\Delta n_{eff}} \quad (3)$$

2 Results and discussion

In this study, the FDTD method is used to investigate the changes of the effective refractive index of two different geometric structures of waveguides (i.e., the rib and strip waveguides) as the ambient refractive index varies. The refractive indices for the Si core and SiO_2 insulator layer used in this paper are 3.42 and 1.46, respectively. All the simulations are based on TE mode and the thickness of SiO_2 insulator is 1 μm. The incident light is at a wavelength around 1.55 μm. Figure 2 shows the effective refractive index change Δn_{eff} as a function of the ambient refractive index n_e of the two waveguides. It can be seen that, for the two waveguides, Δn_{eff} increases with n_e linearly, which agrees well with previous studies[10]. As inspired by the previous study[10], the sensitivity of the sensor is expressed by the sensitivity coefficient

$$K = \frac{\Delta n_{eff}}{\Delta n_e} \quad (4)$$

where Δn_e is the change of ambient refractive index. For a specific design, K is a constant depending on the waveguide structure.

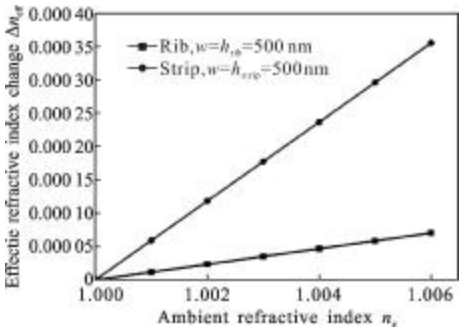

Fig.2 Changes of the effective refractive index as the ambient refractive index increases for the strip and rib waveguides structures, $w=h_{strip}=h_{rib}=500$ nm

For each kind of waveguide, the optimization of design parameters is carried out firstly. To study the effects of the geometry dimension of waveguide on the sensitivity, the cross-sectional area of the waveguide, which can also affect the sensitivity, should be kept constant. The core width dependent sensitivity coefficient **K** of the strip waveguide in the same cross-sectional area is plotted in Fig.3(a). It is shown that the **K** values of the three curves are very low when their widths are relatively narrow (their thickness are relatively high at the same time). The **K** values increase as the widths become larger, and then they all reach their maximum values, of which the width and thickness of the waveguides are (333 nm, 333 nm), (400 nm, 400 nm) and (500 nm, 500 nm) for 0.1 μm^2, 0.16 μm^2 and 0.25 μm^2 curves. That means when the widths are equal to the thicknesses (i.e., $\mathbf{w}=\mathbf{h}_{strip}$, the cross sections are square), the maximum **K** can be achieved. This indicates that a more symmetrical structure has a better **K**. And the **K** values tend to decline as the widths increase further (i.e., the waveguide becomes flatter).

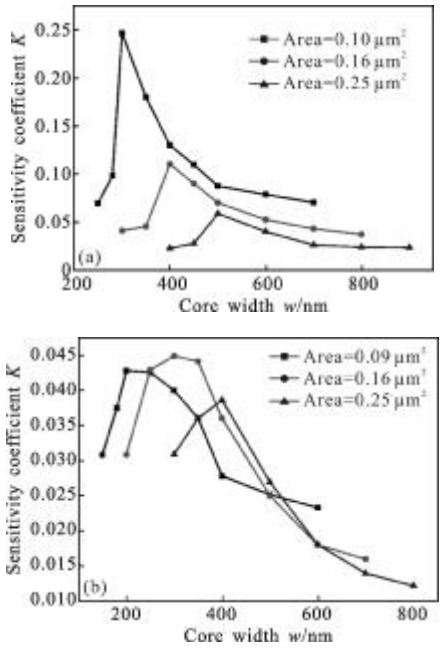

Fig.3 Change of sensitivity coefficient **K** as the core width increases for (a) strip waveguide (b) rib waveguide

Similarly, Figure 3(b) contoured the **K** value as a function of the core width of rib waveguide under the constant cross-sectional area condition. The curves for rib waveguide show the similar trend as those for strip waveguide. When the waveguide is relatively narrow, the **K** value is around 0.03 for these three curves. After that, as the width increases (the thickness drops correspondingly), each curve presents a peak. However, compared with the symmetrical structures under which condition strip waveguide can get preferable performances, these peaks correspond to specific not fully symmetrical structures. Furthermore, it is obvious that strip waveguide with a higher **K** value performs better than rib waveguide. After the maximum point, the **K** value falls with the increase of width.

For the strip waveguide and rib waveguide with the same core thickness ($\mathbf{h}_{strip}=\mathbf{h}_{rib}=200$ nm), Figure 4 shows the **K** value as a function of the core width of these two waveguides, respectively. According to the curves, the sensitivity coefficients of both the strip and rib waveguides decreases with the increase of core width, during which the amplitude change of the strip waveguide is more dramatic. Furthermore, the maximum value of **K** for the strip waveguide can reach 0.141, while that for the rib waveguide can only be 0.031. As the curve of the strip waveguide is always above the rib waveguide curve, it can be concluded that the strip waveguide demonstrates a better sensing performance than the rib waveguide when their dimensions are the same.

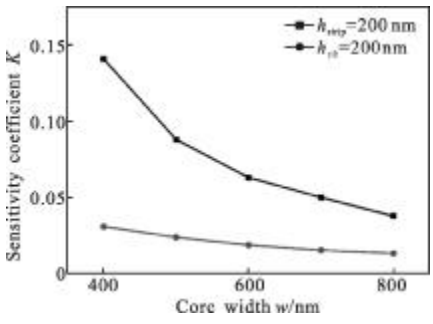

Fig.4 **K** values as a function of the core width of the strip waveguide and rib waveguide

As analyzed above, there is a wide range of factors related to sensitivity for microring resonator

sensors with different cross sections, even if their dimensions are similar. The higher sensitivity could be achieved if the area of cross section with the same width is smaller for strip waveguide. However, state-of-the-art limits the minimum of the area of cross section, so the effective way is to optimize the device structure to improve the sensitivity. Assuming the processing limit of micro-fabrication is 300 nm, the sensitivities of both structures with similar cross-sectional areas are calculated in Fig.5. For the rib structure, the sensitivity of sensor is only 22.3 nm/RIU. For strip structure with the same cross-sectional area, this value could be 121.8 nm/RIU, 5.47 times better than the rib structure. If the strip waveguide is more symmetrical, which means the width is equal to the thickness (i.e., the cross section is square), the sensitivity can reach 172.3 nm/RIU. Therefore, the sensing performance of the strip waveguide is more desirable than the rib waveguide.

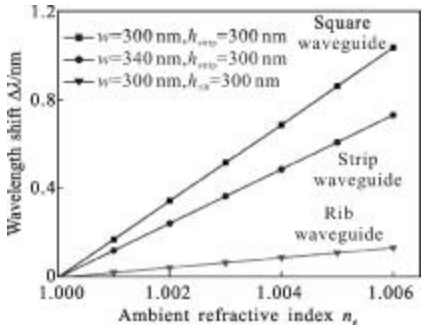

Fig.5 Sensitivities of the microring sensors for strip and rib structures

The reason why the sensing performance of strip waveguide is better than that of rib waveguide can be explained through their mode field distributions. For silicon waveguide with a submicrometer size, there exists strong evanescent wave at the surface of the waveguide, which interacts with the analyte outside the waveguide. When used as a biosensor, the strength of the evanescent field is a crucial indicator for the sensing performance of micro-ring based sensors. The higher the evanescent field strength is, the stronger the interaction between the light and the analyte is, thus the sensitivity is higher [3]. The mode field distributions of strip and rib waveguides with different dimensions are illustrated in Fig.6. For strip and rib waveguides, it can be seen that the optical confinement becomes weaker with the decrease of the waveguides' dimensions within certain range, on the contrary, the evanescent field becomes stronger. Furthermore, by comparing the mode field distributions of the strip and rib waveguides in Fig.6, it's obvious that the evanescent fields at the surface of strip waveguides are stronger than those of rib waveguides in each set of dimensions, which agrees well with the results mentioned before.

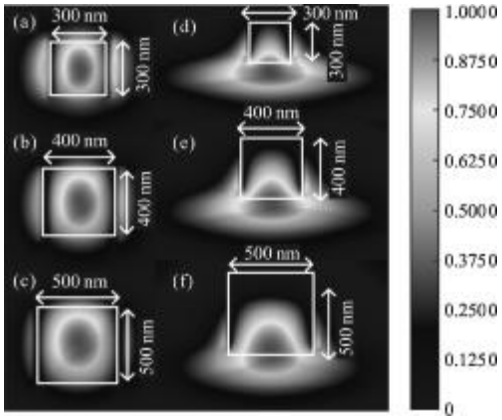

Fig.6 Mode field distributions of the strip and rib waveguides in different dimensions, strip waveguides: (a) $w=h_{strip}=300$ nm, (b) $w=h_{strip}=400$ nm, (c) $w=h_{strip}=500$ nm; rib waveguides: (d) $w=h_{rib}=300$ nm, (e) $w=h_{rib}=400$ nm, (f) $w=h_{rib}=500$ nm

Apart from sensitivity, the optical losses (insert losses and propagation losses) of strip waveguide are higher than those of rib waveguide. The losses are mainly caused by strong light scattering on the sidewall roughness due to the processing, which could be reduced by the processing technology mentioned before. For submicron dimensions, the strip waveguide is very favorable, its advantage is the strong mode confinement, very sharp bends and needless to care about single mode operation. However, the rib waveguide is still of great importance, for unique mode characteristics, low losses and functional flexibility.

3 Conclusion

In this paper, the effects of the cross section geometry and dimension of the waveguides on the sensing performance were investigated in detail. Two kinds of waveguides including rib and strip waveguides were analyzed. Firstly, the cross section dimensions of both waveguides were simulated and optimized, respectively. The simulation results demonstrated that sensitivity strongly depends on the geometry and dimension of the cross section. For strip waveguide, the maximum sensitivity 172.3 nm/RIU is achieved when the waveguide is fully symmetrical in case of the same cross-sectional area. However, the rib waveguide's peak occurs when its geometry is not completely symmetrical. Comparatively, the strip waveguide demonstrated a better sensing performance than the rib waveguide when their dimensions were the same, which is due to their mode field distributions. Furthermore, the sensing performance can be enhanced by improving processing technology. It is revealed that the full-symmetrical structures have great potential to improve the performance of microring resonator sensors in the future.

References:

[1] Chen Xia, Li Chao, Tsang Hon K. Device engineering for silicon photonics[J]. NPG Asia Materials, 2011, 3: 34-40.

[2] Kong Xiaojian, Huang Dexiu, Liu Deming, et al. Research on gradient-index strip waveguide coupler [J]. Infrared and Laser Engineering, 2004, 33(2):204-208.

[3] Bogaerts W, Heyn P D, Vaerenbergh T V, et al. Silicon microring resonators[J]. Laser & Photonics Reviews, 2012, 6(1): 47-73.

[4] Guo Wei, Xu Fei, Lu Yanqing. Coupling influence on the refractive index sensitivity of photonic wire ring resonator [J]. Optics Communications, 2012, 285(24): 5144-5147.

[5] Vlasov Yurii A, McNab Sharee J. Losses in single-mode silicon-on-insulator strip waveguides and bends [J]. Optics Express, 2004, 12(8): 1622-1631.

[6] Carlos Angulo Barrios. Optical slot-waveguide based biochemical sensors[J]. Sensors, 2009, 9(6): 4751-4765.

[7] Yang Gilmo, White Ian M, Fan Xudong. An opto-fluidic ring resonator biosensor for the detection of organophosphorus pesticides [J]. Sensors and Actuators B, 2008, 133(1): 105-112.

[8] Katrien De Vos, Irene Bartolozzi, Etienne Schacht, et al. Silicon-on-Insulator microring resonator for sensitive and label-free biosensing[J]. Optics Express, 2007, 15(12): 7610-7615.

[9] Cho H K, Han J. Numerical study of opto-fluidic ring resonators for biosensor applications[J]. Sensors, 2012, 12(10): 14144-14157.

[10] Dai Danxin, He Sailing. Highly-sensitive sensor with large measurement range realized with two cascaded-microring resonators[J]. Optics Communications, 2007, 279(1): 89-93.

[11] Jia Lianxi, Geng Minming, Zhang Lei, et al. Dispersion characteristics of nanometer-scaled silicon rib waveguides[J]. Chinese Optics Letters, 2010, 8(5): 485-489.

[12] Hung Shihche, Liang Eihzhe, Lin Chingfuh. Silicon waveguide sidewall smoothing by KrF excimer laser reformation [J]. Journal of Lightwave Technology, 2009, 27(7): 887-892.

[13] Passaro V M N, Notte M L. Optimizing SOI slot waveguide fabrication tolerances and strip-slot coupling for very efficient optical sensing[J]. Sensors, 2012, 12(3): 2436-2455.

[14] Jiang Desheng, Liu Er, Chen Xing, et al. Design and properties study of fiber optic glucose biosensor [J]. Chinese Optics Letters, 2003, 1(2): 108.

[15] Li Zhihong, He Duiyan, He Lei. Power loss analysis of transitional waveguide by the finite-difference beam propagation method [J]. Infrared and Laser Engineering, 2004, 33(1): 93-96.

[16] Huang Qingzhong, Yu Yude, Yu Jinzhong. Experimental investigation on submicron rib waveguide microring/racetrack resonators in silicon-on-insulator[J]. Optics Communications, 2009, 282(2009): 22-26.

[17] Reiko Hiruta, Hitoshi Kuribayashi, Ryosuke Shimizu, et al. Flattening of micro-structured Si surfaces by hydrogen annealing [J]. Applied Surface Science, 2006, 252(2006): 5279-5283.

[18] Shi Qiang, Sang Shengbo, Zhang Wendong, et al. Research development of nano optical waveguide smoothing technology [J]. Infrared and Laser Engineering, 2013, 42(11): 3040-3046.

[19] Li Zhigang, Du Zhenhui, Wang Baoguang, et al. Optical fiber temperature sensor based on wavelength-dependent detection[J]. Chinese Optics Letters, 2004, 2(4): 220-222.

[20] Jiang Shaoji, Liang Youcheng, Zhu Xi. Asymmetric fabry-perot interferometric cavity for fiber optical sensors [J]. Chinese Optics Letters, 2006, 4(10): 563-565.

[21] Su Baoqing, Wang Chunxia, Kan Qiang. Compact silicon-on-insulator dual-microring resonator optimized for sensing[J]. Journal of Lightwave Technology, 2011, 29(10): 1535-1541.